Application of Tagged Neutron Method for Diamonds Detection in Kimberlite

Bystritsky V.M., Zubarev E.V., Rogov Yu.N., Sadovsky A.B., Sapozhnikov M.G., Tarasov O.G.

Diamant LLC, Dubna

Introduction

At present standard diamond processing technology implies disintegration of kimberlite ore in crushers or grinding rolls down to a size of 0.2 mm. It inevitably leads to high probability that large and most valuable diamonds could be damaged. The fraction of diamond crystals which lost integrity in the process of ore enrichment could be as large as 35–65% [1].

Tagged neutron method (TNM) [2] offers a possible solution to this problem. It allows detecting diamond inside kimberlite ore without its disruption.

The main idea of the TNM is irradiation of object by fast 14.1 MeV neutrons from binary nuclear reaction

$$d + {}^3H \rightarrow {}^4He + n. \quad (1)$$

By detecting (tagging) the α-particle that accompanies neutron it is possible to determine direction of the neutron. Those tagged neutrons irradiate kimberlite ore under investigation and produce gamma quanta via inelastic scattering reactions with nuclei

$$n + A \rightarrow n` + A^*, \quad A^* \rightarrow \gamma + A. \quad (2)$$

Gamma ray spectra from reaction (2) are unique for every chemical element present in kimberlite. Characteristic γ-rays are registered by γ-detectors in coincidence with the signal from the α-detector. Measurement of the time interval between the signals from the α- and γ-detectors allows determining the distance from the neutron source to the point from which the γ-quantum is emitted since the neutron speed is constant and equal to 5 cm/ns. If one uses a position-sensitive α-detector, then knowing the direction of the neutron and distance from tritium target traveled by the neutron until it produced a γ-quantum, it is possible to restore all three spatial coordinates of interaction point. This allows determining spatial distribution of chemical elements in the irradiated sample.

The tagged neutron method (also called Associated Particle Imaging (API) method) has been widely used [2] in explosives and drug detectors, which allow determining elemental composition of the substance hidden in the examined objects of various sizes from hand luggage to shipping containers.

Diamond detection in kimberlite ore using TNM was demonstrated in [3]. In the following we discuss the results of field testing of the prototype of the neutron separator. The tests were done on kimberlite ore of Lomonosov deposit in June-September of 2015 at enrichment plant Pomorskaya of PJSC Severalmaz.

Description of the setup

The general scheme of the setup is shown in Fig.1. The kimberlite ore is loaded in feeding hopper and via tray-based feeding system is supplied to the inspection zone of neutron module. In neutron module the ore is irradiated by the fast 14 MeV neutrons. As the source of fast neutrons a portable neutron generator is used. It is installed under the conveyer belt. Above the belt is the gamma-detector module for detecting the characteristic gamma-radiation induced by the fast neutrons. After analysis of obtained gamma-ray spectra the decision making software produced a signal to move inspected portion of ore either to the tailings or to the concentrate bunkers.

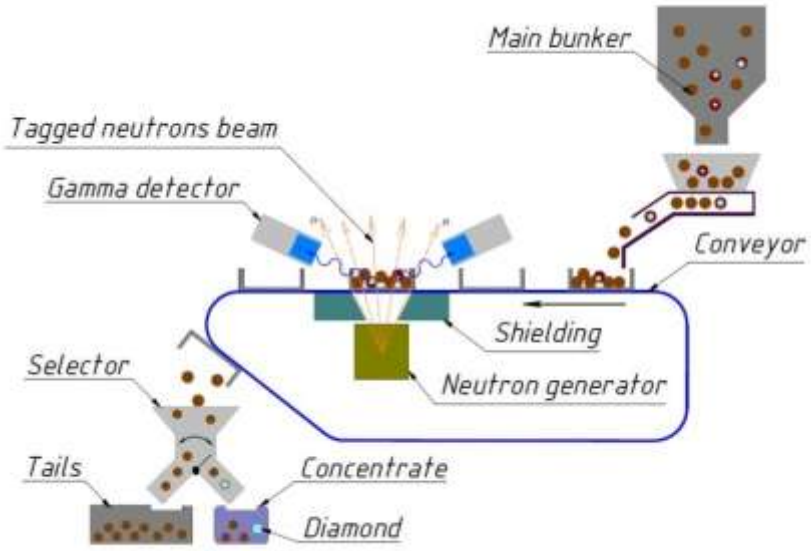

Fig. 1. General scheme of the setup.

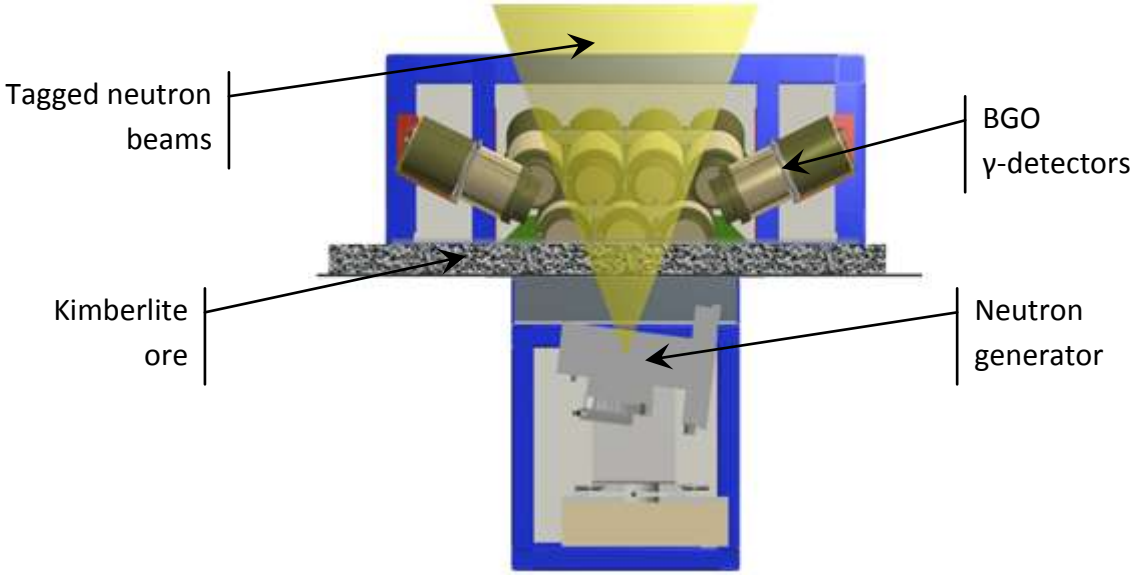

Fig. 2. General scheme of the neutron module.

Schematic view of the neutron module is shown on Fig.2. At the bottom of the neutron module there is a neutron generator with a built-in 192 pixels alpha-detector. The box with 14 BGO gamma-detectors is above the conveyer belt.

Neutron generator with built-in 192 pixel alpha-detector

The neutron generator ING-27 shown in Fig.3 is designed and produced by the Dukhov All-Russia Research Institute of Automatics, Moscow. Neutron generator produced a continuous flux of 14.1 MeV neutrons with intensity $I=5\times10^7$ s^{-1}. The size of the generator is 292×199 ×279 mm, mass of neutron generator is 8.8 kg, and power consumption is 40 Wt.

Uniqueness of the designed generator lies in a 192-pixel built-in silicon based alpha-detector. 192-pixel alpha-detector is a 12×16 matrix of 6×6 mm silicon pixels. The distance between pixel centers is 7 mm, with total sensitive area of alpha-detector of 72×96 mm. The distance from alpha-detector to tritium target is 100 mm.

To our knowledge, 192-element alpha-detector is one of the best used for the TNM technique. Comparison of different alpha-detectors is given it Table 1.

Table 1. Characteristics of different alpha-detectors

Type of neutron generator	Number of tagged beams	Size of the pixel, mm	Spacing between pixels, mm
ING-27 [4]	9	10	0.1
Sodern, Euritrack [5]	64	5.8	0.2
API-120 [6]	25	3	–
ING-27 [3]	64	4	–
Present work	192	6	1

192-pixel alpha-detector allows forming a tagged neutron inspection zone, which is larger by a factor of 3.5 than inspection zone of standard 9-pixels ING-27 neutron generator of VNIIA [4].

Fig. 3. ING-27 – neutron generator with built-in 192 pixel alpha-detector.

Spatial characteristics of tagged neutron beams have been evaluated by a specially designed scintillating strip profilometer, consisting of two perpendicular planes of 16 strips each. Size of each strip made of plastic scintillator is 150×7.5×5 mm. All 16 strips on each plane of profilometer are light-insulated. Light collection to a multianode photomultiplier is done via fibers. Approximation of measured spatial distribution of nine adjacent tagged beams corresponding to X-strips of alpha-detector is shown on Fig.4. Measured distributions were approximated by Gaussian function with a linear background. One can clearly see that tagged beams overlap, with visible gaps between them. As expected, the central tagged beam has the highest amplitude, and the amplitude of peaks declines from inner to outer beams. This variation of amplitude is connected with the fact, that strips of alpha-detector of equal area are visible from the tritium target at different spatial angles, with central strip covering the most of solid angle because it is the nearest to the tritium target.

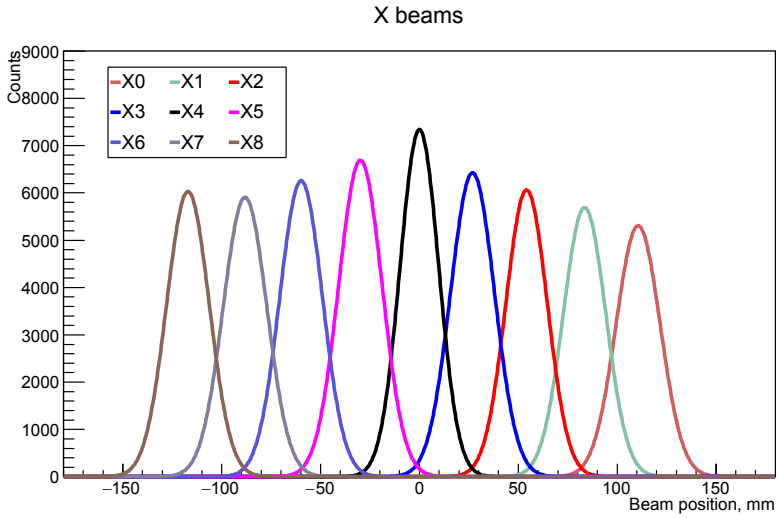

Fig.4. Approximation of measured spatial distribution of nine adjacent tagged beams corresponding to X-strips of alpha-detector.

Alpha-detector cells had width d=6 mm, and distance from tritium target to alpha-detector was r = 100 mm. Then, assuming a point-like deuteron beam, the size D of tagged neutron beam at distance R = 420 mm from tritium target should be D = dR/r = 25.2 mm, while averaged measured FWHM is 25.2±0.1 mm. Therefore, results of spatial measurements of tagged beams are in a good agreement with the values expected from a point-like deuter hitting the target. That is important feature of this neutron generator.

Gamma detectors

Detection of gamma-rays produced from ore irradiation by fast neutrons is performed by a system of 14 gamma-detectors based on BGO crystals with a diameter of 76 mm and thickness of 65 mm. These detectors have high efficiency of gamma rays detection within the energy range of interest and low efficiency of background neutrons detection.

Measurement of energy resolution of gamma-detectors and time resolution of α-γ coincidence system had been estimated with measurement of 4 cm thick carbon plate. Measurement has been done at intensity of neutron flux of 3.3×10^7 n/s. Average gamma-detector load at this intensity and amplitude threshold of 1.5 MeV is 45×10^3 pulses/s. For

estimation of energy resolution, energy spectra from every individual gamma-detector are calibrated and summed up together. The resulting spectrum is approximated with the sum of two Gaussians and parabola (Fig.5). The energy resolution of gamma-detector system at energy 4438 keV is Γ=4.39±0.03%.

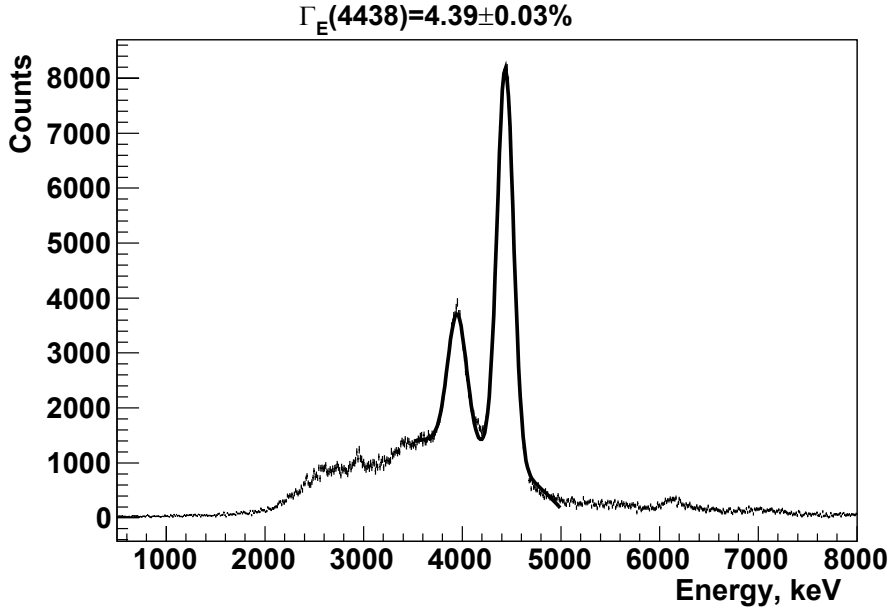

Fig.5. Total energy spectrum of carbon sample.

A time spectrum of α-γ coincidence system with an additional cut on energy of registered γ-quanta applied is shown on Fig.6. Applied cut isolates the energy region containing 4438 keV peak of ^{12}C. As one can see, spectrum exhibit contribution of random coincidence events represented by flat component of shown distribution and noticeable coincidence peak.

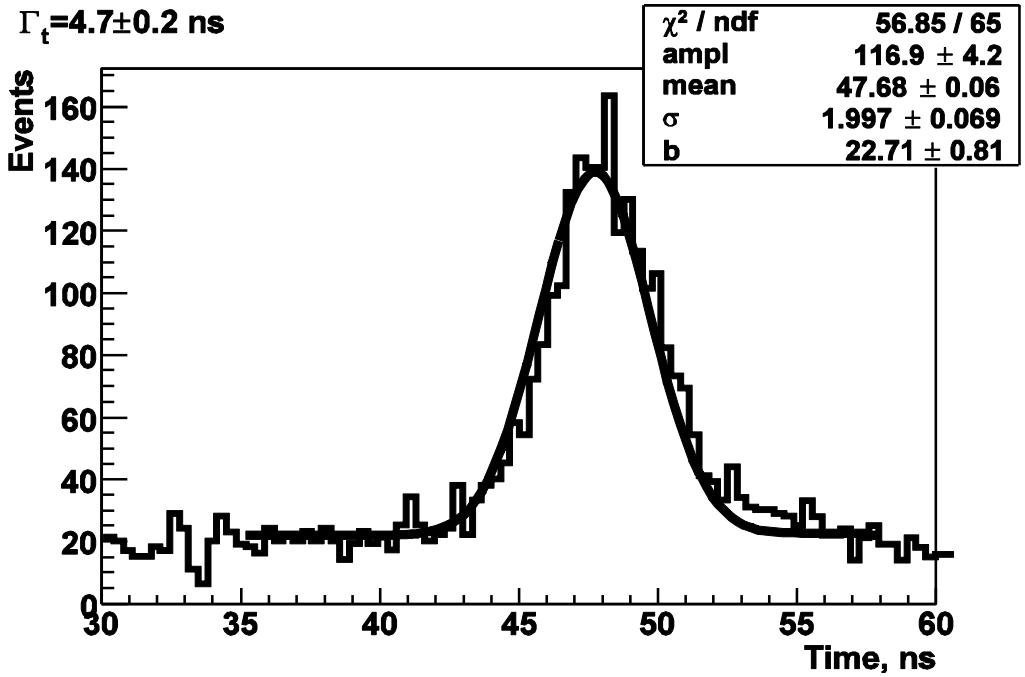

Fig.6. Time spectrum of α-γ coincidence for carbon sample for coincidence between γ-channel №8 and α-channel №3 is approximated by a Gaussian and flat background.

The time resolution Γ_t of alpha-gamma coincidence system at intensity of neutrons 3.3×10^7 n/s is $\Gamma_t = 4.7 \pm 0.2$ ns.

Data acquisition system

The recording electronics of the data acquisition system for the alpha- and gamma-detectors is designed as a single board, which has the size of a standard PCI card and can be inserted in a PCI-E slot of a personal computer. The hardware data acquisition board utilizes high-speed ADC for sampling of input signals. The system of registration process signal from alpha- and gamma-detectors is based on the principle of waveform-digitizing with subsequent calculation of their time and amplitude characteristics.

Channels of digitizing signals from the detectors are built on the same scheme, which includes an amplifier with 0–20 MHz band-pass filter and ADC measurement interval of 10 ns (100 MHz). The digital code corresponding to each measurement is fed to ADC programmable logic circuit, in which the definition of moments of (α-γ)-coincidences is performed in digital form.

Programmable scheme logic of the electronics board of DAQ system organizes the reception of information from the ADC, allocates of coincidence moment definition, prepares a data buffer and provides its transfer to PC memory. Subsequently the exact value of the pulse amplitudes and the time interval between them are calculated.

The special software for selection and signal processing extracts information about (α-γ)-coincidence, determines triggered channel numbers, calculates a time interval between pulses and the area under the pulse envelope, defining thereby an amount proportional to the energy released in the detectors, and counts the pulses detected by each detector individually. These parameters are presented in real-time histograms and stored in the data file.

Power supply and slow-control

Slow control system uses ADC PC card connected to voltage monitoring outputs of every power supply, and to current monitoring output of alpha-detector high-voltage power supply. Also thermocouples for monitoring temperature of gamma-detectors, neutron generator, data acquisition system and internal temperature of equipment rack were used to control the temperature conditions.

Slow control system was incorporated in the operator's GUI and displayed operability of every main system of the setup, i.e. gamma-detector unit, neutron generator unit, power supply unit, communication lines etc. Operability was displayed in simplified OK/not-OK view, with additional detailed information about detected failures in tooltip frames. Failures were detected by testing current measured parameters against pre-defined reference values and by monitoring contents of log-files supplied by software modules.

In order to compensate a thermal dependence of BGO crystals, an energy response of every gamma-detector was corrected in accordance with its measured temperature [7].

Measurement results

Characteristic gamma-ray spectrum of carbon isotope ^{12}C is very simple (Fig.5). It features a prominent peak at 4438 keV energy with a single escape peak offset by 511 keV followed by Compton scattering tail. This simple shape of carbon spectrum facilitates detection of carbon signal in gamma-ray spectra obtained by irradiation of kimberlite ore

samples. Since diamonds consist of pure carbon, the technique for diamond detection in kimberlite sample is reduced to detection of carbon excess in a particular area of the sample.

For testing the setup operation we used core samples from Karpinskogo and Arkhangelskaya mines. Depth at which these samples were obtained varied from 35 to 110 meters. The spectra of the samples are shown in Fig.7. We intentionally cut low energy part of spectrum to decrease the data flow, and because of that in Fig.7 all main visible peaks are oxygen nuclei, with some admixture from calcium at 3800 keV peak. For the samples from Karpinskogo mine, a small peak of carbon is seen at approximately 4440 keV, while the content of carbon in the samples from Arkhangelskaya mine is smaller.

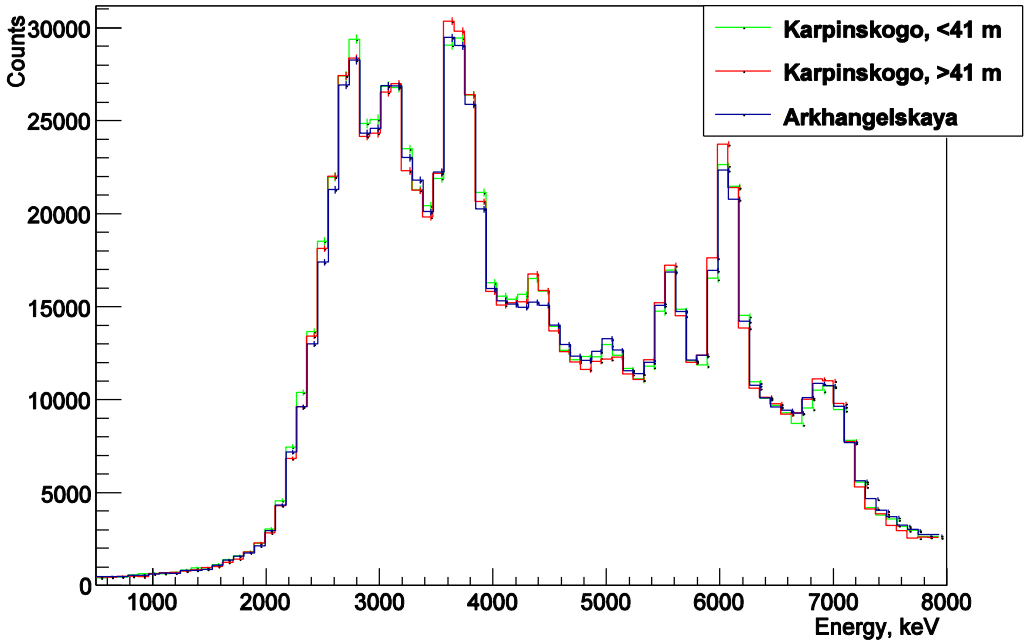

Fig.7. Energy spectra of investigated core samples from different sources.

For tests we split the ore rocksin two halves and put a diamond simulant in between. Diamond simulants are glued cylinders of artificial diamond sand. The height of a cylinder is equal to its diameter. Simulants of 6, 8, 10, 12 and 14 mm with typical density of 2.44 ÷ 2.48 g/cm^3 were used. Rocks with diamond simulants were 50 mm, 40 mm and 30 mm in size. Those rocks were mixed with kimberlite ore.

Detection procedure was the following. A tray with ore was divided by tagged neutron beams into 192 regions with the region size about 8×8 mm. In each cell a local carbon level was evaluated and compared to the carbon level averaged over sample.

Fig.8 shows gamma-spectra from an experiment with irradiation of 8 mm diamond imitator inserted in the kimberlite ore sample of 50 mm size and surrounded by ore samples of the same size. Red points with error bars represent gamma-ray spectrum for tagged beam irradiating diamond simulant location, while black histogram represent spectrum of ore sample averaged over all tagged neutron beams. The local carbon signal excess is a clear indication of presence of diamond imitator in the selected tagged neutron beam.

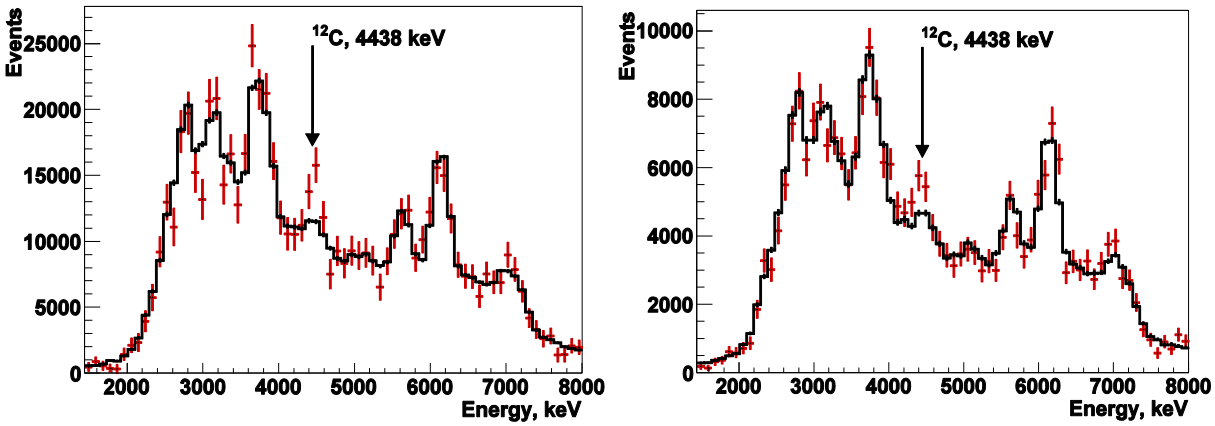

Fig. 8. Gamma-ray spectrum 8 mm diamond imitator in 50 mm kimberlite ore (left). Similar figure for 14 mm diamond imitator in 160×90×90 mm kimberlite ore rock (right). Points with error bars represent gamma-ray spectrum for tagged beam irradiating diamond simulant location. Histogram represents spectrum of ore sample averaged over all tagged neutron beams.

One of the advantages of TNM is high penetration ability of 14 MeV neutrons and high penetration ability of resulting 4 MeV gamma-rays. This allows investigating relatively thick ore samples. The largest analyzed rock had size of 160×90×90 mm, and with this rock we used 14 mm diamond simulant, which we put approximately in the geometrical center of the rock. Corresponding comparison of spectra is on right side of Fig.8. One can see, that even for 10:1 ore to diamond size ratio a clear excess in the carbon peak region is visible.

In total 281 measurement with different imitator sizes and 1416 measurements with empty ore samples were taken. The throughput of the prototype was 102 kg/hour for ore size 50mm. The concentrate yield (a fraction of ore with positive response of the detection procedure) was 3%. The diamond detection probability was calculated to be 97%. The largest operable ore size was 150 mm.

Radiation control is a crucial part of the setup operation. Measurements of radiation environment during setup operation at operator location gave the value of 0.11 μSv/h. Induced activity of core sample after irradiation was 0.17 μSv/h. In a transport container the radioactive background was 0.11 – 0.17 μSv/h with neutron generator switched off while natural radioactive background at operation location at Pomorskaya GRE was 0.09 – 0.11 μSv/h.

Conclusions

Field testing of prototype of neutron separator used TNM was done in June-September of 2015 analyzing kimberlite ore of Lomonosov deposit at Enrichment Plant of Pomorskaya GRE, PJSC Severalmaz. All systems of the neutron module have been operating correctly. Neutron generator operation time was 218 hours without any significant problems. Average power consumption was calculated to be approximately 500 Wt.

In total 1416 measurements with kimberlite ore and 281 measurements with diamond imitators installed in kimberlite ore of different size grades have been taken. It was demonstrated that it is possible to see the diamond in the rock which size is 10 times larger than the size of the diamond.

At present with support of “Skolkovo” Foundation the design and manufacturing of neutron separator with 1 t/h throughput is been carried out. It should be tested this year at Severalmaz Lomonosov deposit.

We want to express our gratitude to Skolkovo Foundation for financial support and for PJSC ALROSA for support in conducting tests and interest in our technology.

We want to express our gratitude to Skolkovo Foundation and to S.A. Zhurbafor financial support in building setup prototype, to PJSC ALROSA administration represented by I.V. Sobolev, A.S. Chaadaev, V.A. Karnatsky, G.M. Nikitinfor support in conducting tests, to PJSC Severalmaz administration represented by A.V. Pismenny, I.I. Ivanov, V.V. Kolenchenko, A.V. Yamov for help in organizing of tests, to Dukhov VNIIA (Moscow) staff members E.P. Bogolyubov, Yu.K. Presnyakov, V.I. Ryzhkov, T.O. Khasaev, D.I. Yurkov for creation of the neutron generator with unique parameters, and also for PJSC Severalmaz staff members R.R. Garifullin, L.N. Burmistrova for continuous support in carrying out the tests.

References

1. **В. А. Карнацкий** и др., Повышение качества товарной продукции АК «Алроса» за счет улучшения технологии раскрытия алмазов, Обогащение руд, №6, 2012г.
2. **V. Valkovic**, 14 MeV Neutrons: Physics and Applications, ISBN-13: 978-1482238006.
3. **V. Alexakhin** et al., Detection of Diamonds in Kimberlite by the Tagged Neutron Method, Nuclear Instruments and Methods A**785** (2015) 9.
4. **V.M. Bystritsky** et al., Physics of Particles and Nuclei Letters, **5** (2008) 441.
5. **S. Pesente** et al, Nucl.Instr.Meth. B**261** (2007) 268.
6. **J. Michalzo** et al, Proc. Int. Conf. Portable neutron generators and technologies on their basis, All-Russia Research Institute of Automatics-VNIIA, (Editor-in-chief: Barmakov, Yu.N.), Moscow, 2012, p.198-212.
7. **V. M. Bystritsky** et al., Gamma Detectors in Explosives and Narcotics Detection Systems, Physics of Particles and Nuclei Letters, 2013, Vol. **10,** No. 6, pp. 566.